DOI: 10.17277/amt.2016.01.pp.009-016

Mathematical and Physical Modeling of the Rolling Process of Tapered Shafts for Aviation Purposes

R.Yu. Sukhorukov[a], A.A. Sidorov[a], A.I. Alimov[a], M.I. Nagimov[b], F.Z. Utyashev[b]*

[a] *A.A. Blagonravov Institute of Mechanical Engineering of the Russian Academy of Sciences (RAS IMASH), Moscow*
[b] *Institute of Metals Superplasticity Problems of the Russian Academy of Sciences (RAS IMSP), 39, Khalturina St., Ufa, 450001, Bashkortostan Republic*

* Corresponding author: Tel.: + 7 917 488 86 69. *E-mail*: imsp@anrb.ru

Abstract

One of the most promising methods for manufacture of axially symmetric parts such as disks or hollow shafts of gas turbine engines is local deformation using cold rolling. Physical and mathematical modeling can be quite effective for designing this class of equipment and process operations. This article presents the methodology and results of physical and mathematical finite element modeling of local deformation of parts such as a tapered cylinder fabricated from chromium steel alloy grade 11H11N2V2MF-Sh. Chemical elements in the alloy are designated by the letters which stand for: H – Chromium, N – Nickel, V – tungsten, M – molybdenum, F – vanadium, Sh – electroslag remelting. According to GOST 5632-72 (Russian standard), this type of nickel-chromium alloy consists of about 11 % of chromium, 1.5–2 % of tungsten and nickel, up to 1 % of molybdenum and vanadium, and 0.11 % of carbon, hundredths of one percent of phosphorus and sulfur. It is heat-resistant high-grade steel, which is used for the manufacture of parts operating unloaded at 900–1000 °C. The purpose of the paper is to analyze the process energy-power parameters and possible fracture of parts during deformation.

Keywords

Isothermal forging; rolling; finite element analysis.

Introduction

Tapered shafts and their combination with discs are essential parts in the design of modern aircraft gas turbine engines. These parts are operated under extreme force and temperature, and therefore are made of heat-resistant alloys based on nickel, iron and titanium.

Currently, punching or forging are the processes that are generally used in the manufacture of tapered shafts. Punching requires the use of powerful hydraulic presses and very strong and bulky dies. High pressure, causing significant deformation during heating, combined with a significant non-uniformity of the field of the accumulated deformation arising due to uneven flow of metal in the die, results in substantial heterogeneity of the structure of parts, and as a consequence, a significant non-uniformity of their properties, such as strength and heat resistance. It should be noted that molds for manufacture of such parts are of low resistance. Forging for the manufacture of shafts is a very laborious process, which does not result in a homogeneous structure due to uneven distribution of accumulated deformation; at the same time it leads to large losses of material, which drastically reduces materials utilization rate (**MUR**).

A method of local deformation [1] significantly increases the degree of homogeneity of the metal structure, reduces the degree of deformation and increases MUR when manufacturing tapered shafts.

Fig. 1 shows a schematic diagram of the cylinder tapered shaft manufacturing process. The process may include forced wall thinning of the workpiece, and in this case the process is called rolling. When wall thinning of the workpiece is not required, the considered process is called rotary drawing. A detailed classification of the processes based on the use of local deformation is presented in [2].

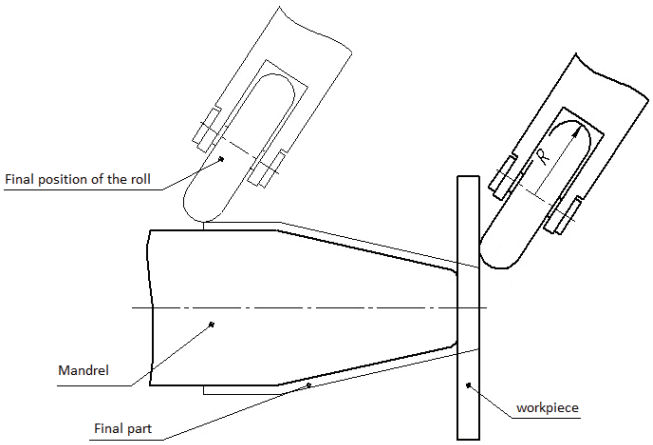

Fig. 1. A schematic diagram of the cylinder tapered shaft manufacturing process

The purpose of this work is to investigate the possibility of manufacturing a hollow shaft with a tapered cylinder from chromium steel alloy grade 11H11N2V2MF-Sh, using physical and numerical modeling, and determine the necessary power parameters for rolling.

Experimental

Rotary drawing of a hollow shaft with tapered cylinder was carried out on PNC-600 Leifeld with pre-heating of workpiece and mandrel in quasi-isothermal conditions. The workpieces were made of sheet material of the above-mentioned alloy with a thickness of 12–16 mm.

The results of physical modeling showed that the most difficult problem to be solved in the design process is to avoid fracture at the junction between the flat and the conical parts of the shaft (attaching point of the workpiece between the clamp and the mandrel). The thinner is the initial workpiece, the greater is the probability of strain localization and parts breakdown in that location (Fig. 2).

A method of numerical modeling

Numerical modeling of the local strain was used in [4–7]. Mathematical model of rolling shafts from high-temperature alloys under isothermal, including superplastic deformation is based on solving the system of the following equations [8]:

– differential equations of equilibrium relating the components of the stress tensor that determines the stress state of the body;

– kinematic equations relating the components of the strain rate tensor and the velocity of the material points of the body;

– Levy-Mises equations of plastic flow relating the stress and strain states of the body, the condition of incompressibility, and Mises plasticity condition;

– a rheological model of the material;

– model of friction between the workpiece and the tool. The solution to this system of equations is carried out by the finite element method using SFTC DEFORM software.

It should be noted that in the case of constructing a model in axisymmetric formulation that does not require significant computing resources, it is better to use a method in Lagrange variables, which is traditionally used for modeling metal forming [9], while in the case of constructing a three-dimensional model it is better to use an Arbitrary Lagrangian Eulerian (**ALE**) formulation of the problem [10], which greatly accelerates the process of modeling.

Results of numerical modeling

In order to determine strength parameters of the manufacturing process of a hollow shaft with tapered cylinder we constructed a three-dimensional model of the rolling process, shown in Fig. 3.

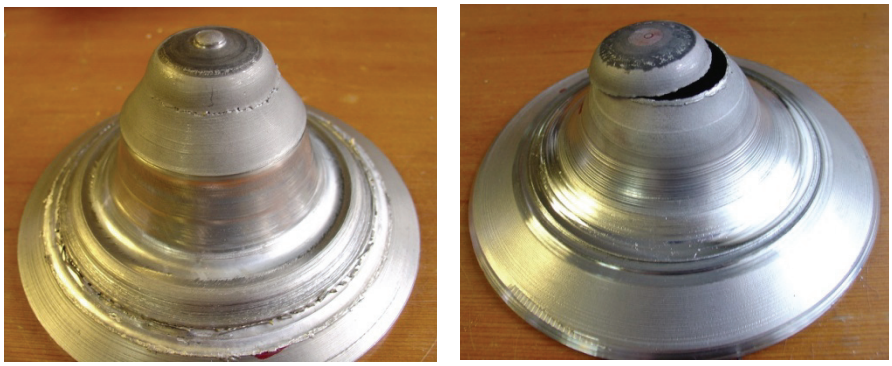

a) *b*)

Fig. 2. Workpiece fracture at the junction of flat and conical parts:
a – strain localization and the beginning of fracture;
b – workpiece fracture

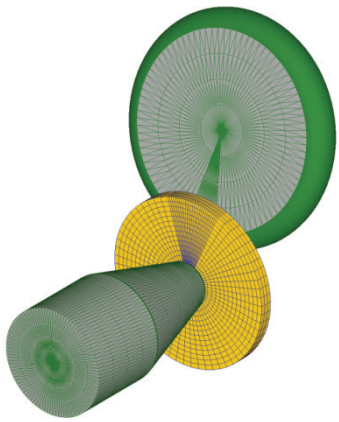

Fig. 3. A three-dimensional model of the rolling process for a hollow shaft with tapered cylinder using DEFORM software

The initial thickness of the workpiece was taken as 20 mm, the diameter was 220 mm. The wall thickness of the final part was 7 mm, i.e. the process involves a considerable thinning of the walls. When calculating we used a rheological model for steel alloy grade 11H11N2V2MF-Sh at a constant temperature of 1100 ° C in the form of:

$$\sigma_s = A\,\varepsilon^u\,\dot{\bar{\varepsilon}}^z + \sigma_0, \qquad (4)$$

where σ_s is material flow stress; A, u, z correction factors of the equation; ε is accumulated strain; σ_0 is material flow limit; $\dot{\bar{\varepsilon}}$ is strain rat.

Coefficients of the rheological model (1) and other basic data of the constructed model are presented in Table. 1.

As can be seen from Fig. 3, in order to accelerate the calculation we used an eight-node hexahedral finite element mesh (6600 elements) of the first order with the local seal in the deformation zone. The calculation on PC equipped with Intel Core i7 processor 2600 3.4 GHz and 8 GB of RAM took 207.6 hours.

The result revealed that the maximum deformation force in the course of rolling occurred at the initial moment, i.e. the workpiece was intensively deformed at the junction between flat and conical parts, and equaled 135 000 N in the axial direction and 101 000 N in the radial direction.

In the study of the causes of failure at the junction between the flat and conical parts we assumed axially symmetric stress-strain state of the workpiece. This assumption was necessary because of the considerable time required to calculate this problem in a three-dimensional setting. It should be noted that this assumption does not take into account the real strain localization (a ring form of the deformation zone in the case of an axially symmetric setting and a spot in the real rolling process), and the possibility of "twisting" the various layers of the cone relative to each other. At the same time modeling of the process in axisymmetric setting shows the similarity of the nature of the metal flow compared with a three-dimensional setting (Fig. 4). In addition, it is clear that in this case fracture is caused mainly by the axial tensile stress, the distribution of which should not change when switching from a three-dimensional setting to an axisymmetric one. Based on all of the above it was assumed that the problem of the risk of fracture at the junction between flat and conical parts was axisymmetric.

In order to study the causes of the fracture at the junction between flat and conical parts of the workpiece in the process of rolling the shaft we analyzed the effect of the original thickness of the workpiece on the likelihood of fracture, and the stress-

Table 1

The main input data for constructing a model of the rolling process

Preset parameter	Value
Coefficients of the rheological model for 11X11H2B2MΦ-Ш	
σ_0, MPa	34
A	76
u	0
z	0.16
Angular velocity of mandrel rotation, rev/min	60
Axial linear velocity of the roller, mm/s	1.17462
Radial linear velocity of the roller, mm/s	0.427525
Siebel friction coefficient	0.7
Amonton-Coulomb friction coefficient	0.25

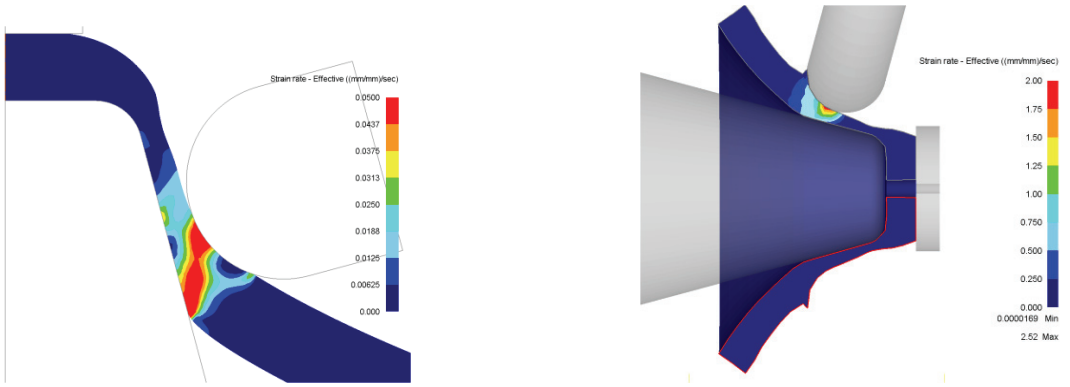

a) *b*)

Fig. 4. Distribution of deformation velocity:
a – for axisymmetric setting; *b* – for three-dimensional ALE setting

strain state at the fracture by using four fracture criteria:

1) The Cockcroft-Latham criterion [11]:

$$D = \int \frac{\sigma^*}{\bar{\sigma}} d\varepsilon, \qquad (2)$$

where σ^* is the maximum principal stress; $\bar{\sigma}$ is material flow stress; ε is accumulated deformation;

2) The Zhao-Kuhn criterion:

$$D = \sigma^* / \bar{\sigma}; \qquad (3)$$

3) the ratio of the maximum principal stress to the tensile strength of the material:

$$D = \sigma^* / \mathrm{UTS}, \qquad (4)$$

where UTS is the ultimate tensile strength of the material;

4) triaxial stressed state:

$$D = \sigma_m / \bar{\sigma}, \qquad (5)$$

where σ_m is the mean stress.

The Cockcroft-Latham fracture criterion is widespread in the analysis of fractures in metal forming and used by the authors all over the world [12–14]; today it is one of the most common fracture criteria in the analysis of the material plasticity resource. At the same time, it should be noted that this criterion does not take into account the material properties relaxation that occurs during the rolling process when the material is not in the deformation zone, i.e. for the analysis of the possibility of the destruction of the workpiece during the rolling process the strength criteria are more suitable (Eq. (3) – (5)), which take into account only the nature of the stress state, rather than the history of deformation.

Fracture models were integrated into the DEFORM post-processor using the custom programming language Fortran 77. The Cockcroft-Latham fracture criterion was integrated into DEFORM software package by its developer, so it was not necessary to integrate it into DEFORM. In addition, due to the fact that the standard functionality of software DEFORM does not allow for the display of all three components of the principal stresses needed to calculate of all four fracture criteria, by using custom programming we calculated principal stresses in the workpiece. The calculation of the principal stresses for a given stress tensor was made using a standard methodology for solutions on the basis of Cardano's formulas.

Fig. 5 shows the results of the developed subprogram.

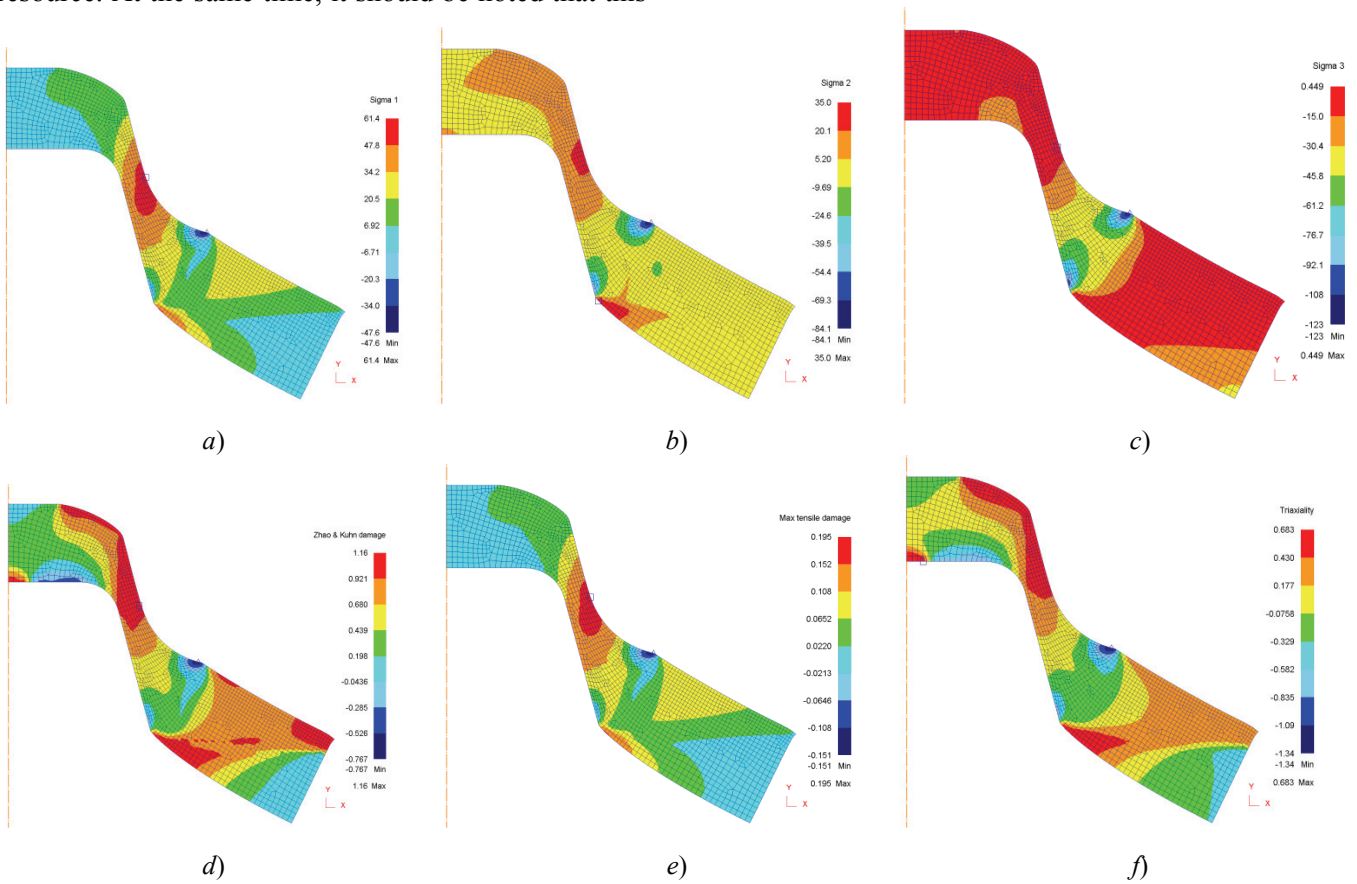

a) *b*) *c*)

d) *e*) *f*)

Fig. 5. The results of custom programming for the rolling process using the workpiece *H* = 30mm:
a – maximum principal stress; *b* – mean principal stress; *c* – minimum principal stress; *d* – the Zhao-Kuhn criterion; *e* – the ratio of the maximum principal stress to the tensile strength of the material; *f* – triaxial stressed state

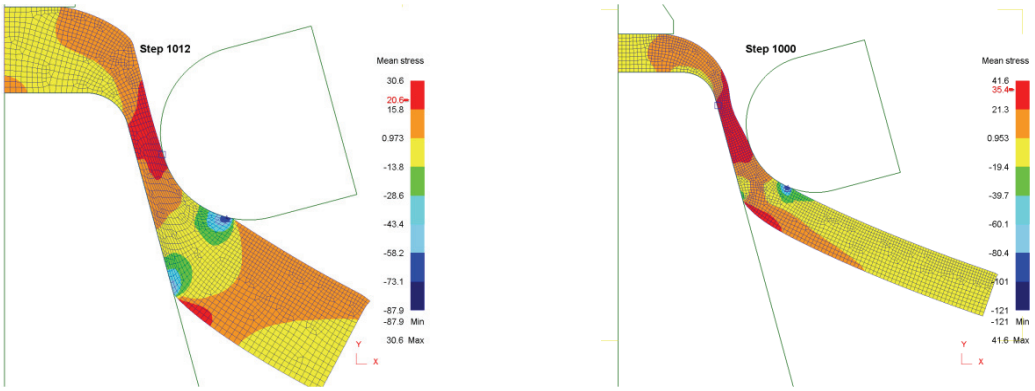

a) *b*)

Fig. 6. Mean stress distribution in the cross section of a workpiece:
a – at a thickness of the workpiece $H = 30$ mm; *b* – at a thickness of the workpiece $H = 16$ mm

Simulation showed that with increasing thickness of the initial workpiece the likelihood of fracture decreased; in particular Fig. 6 shows that in the case of a thicker initial workpiece the material has less tendency to thinning at the junction between flat and conical parts.

For a deeper analysis of the causes of the fracture at the junction between flat and conical parts of the workpiece we conducted four experiments followed by a numerical analysis of the stress state in the zone of plastic deformation for each of these experiments. We considered four different workpieces with thickness: $H = 16, 20, 25, 30$ mm, respectively. Table 2 shows the indicators characterizing the state of stress of the deformation zone and fracture criteria for the above material.

The analysis of the workpiece stress state showed that with an increase in thickness of the workpiece, the maximum principal stress σ_1 decreased, while the minimum principal stress σ_3 gradually changed from positive (tensile) to negative (compression), which entailed a reduction in the mean stress and a positive impact on the resource plasticity in the deformation zone.

For further analysis of the rolling process of these parts it is advisable to determine the critical values of fracture criteria for this process, as well as the shape of the workpiece and a deforming tool (roller). At the same time, all three strength fracture criteria showed a decrease in the probability of fracture with increasing thickness of the original workpiece.

For conical parts with a small cone angle $2\alpha < 30°$, a pre-deformed workpiece similar in shape to the desired product should be used as the initial workpiece. In our case, $2\alpha = 30.6°$, which is close to the minimum permissible value. Thus, for the subsequent numerical simulation we selected a workpiece conical in shape with an angle of 45°; the results of numerical modeling are shown in Fig. 7.

Table 2

The results of the analysis of stress state and plasticity resource (fracture criteria)

Workpiece thickness H, mm	Principal stresses			Mean stress	Fracture criteria			
	σ_1	σ_2	σ_3	σ_m	$\sigma^*/\bar{\sigma}$	$\int \frac{\sigma^*}{\bar{\sigma}} d\varepsilon$	σ^*/UTS	$\sigma_m/\bar{\sigma}$
16	74.0	39.9	3.4	39.1	1.210	1.020	0.208	0.640
20	62.6	32.1	3.27	32.7	1.200	1.060	0.199	0.635
25	52.4	19.6	–11.4	20.2	0.936	0.953	0.166	0.362
30	51.4	16.1	–17.7	16.6	0.858	0.882	0.163	0.277

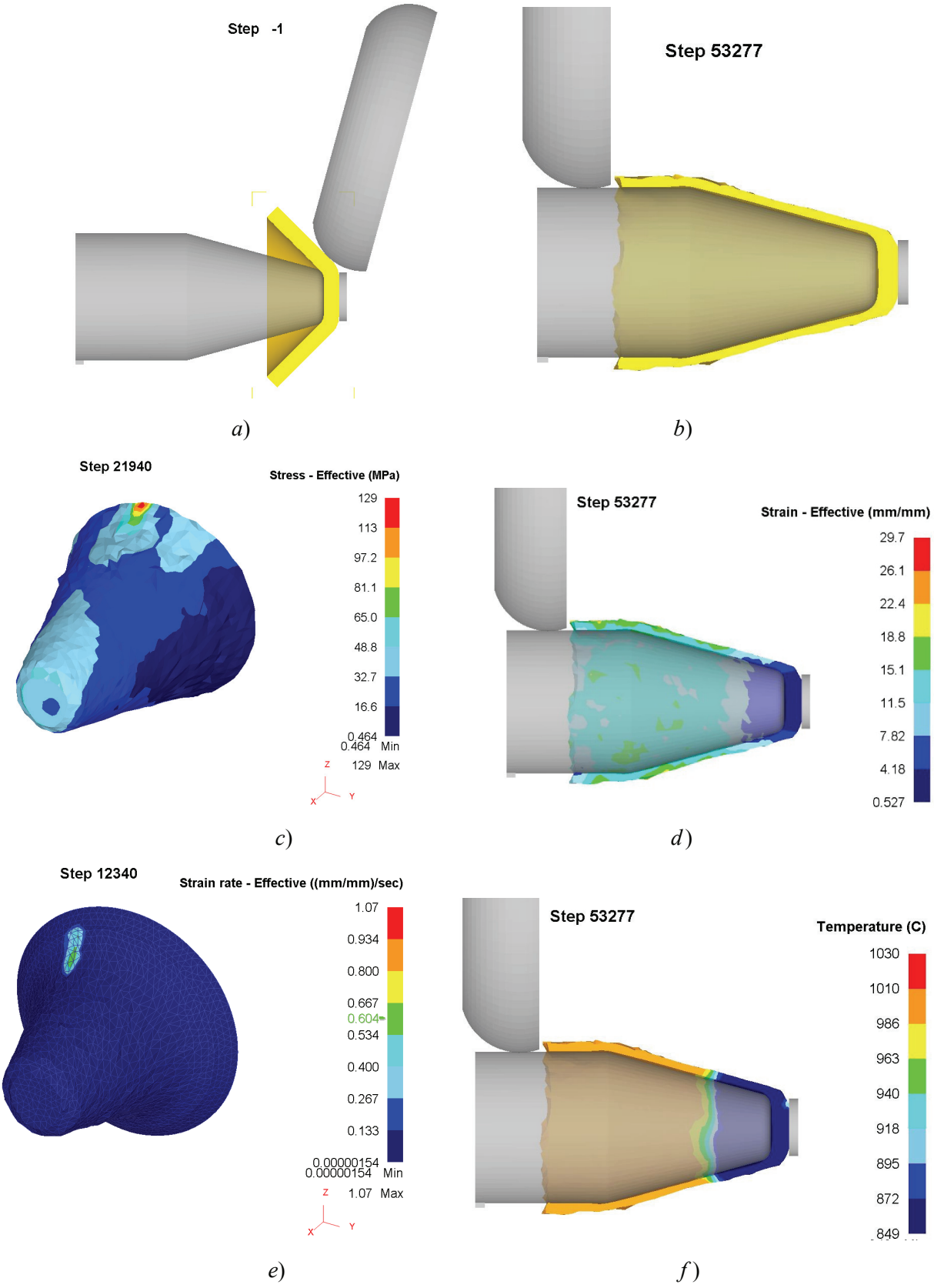

Fig. 7. The results of numerical modeling for a cone-shaped workpiece with an angle of 45°:
a – position of the workpiece and the tool at the initial time; *b* – shaft model after rolling;
c – distribution of stress intensity; *d* – distribution of deformation intensity;
e – distribution of deformation velocity; *e* – distribution of temperature field

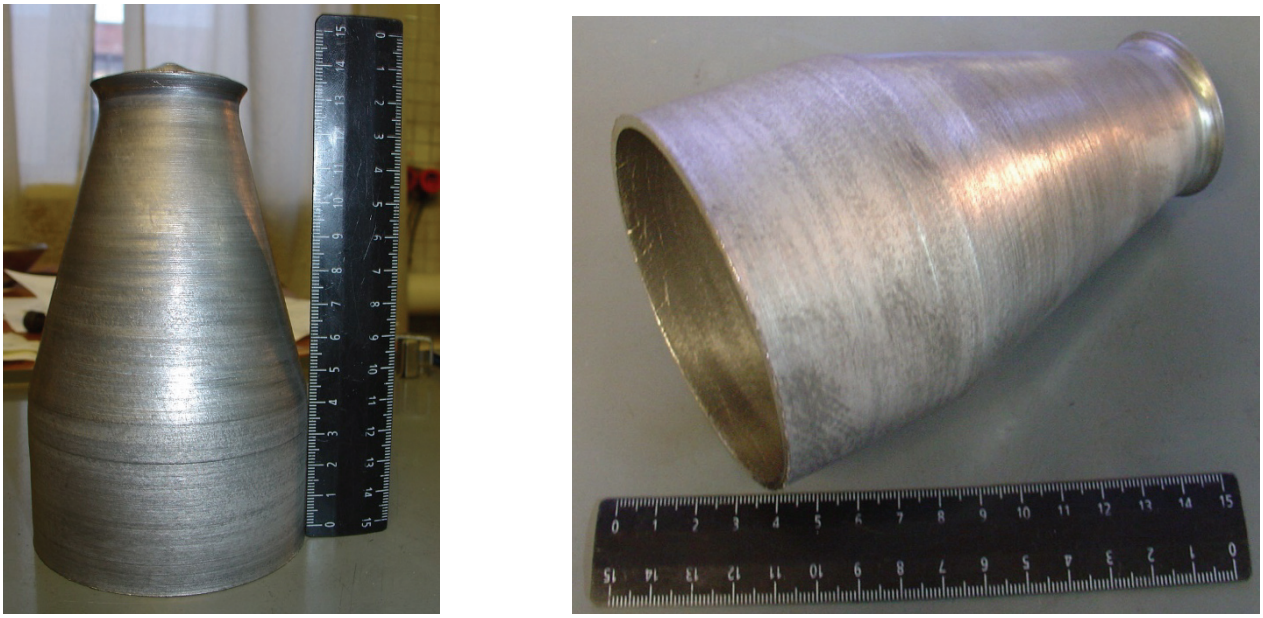

a) *b*)

Fig. 8. The results of physical modeling:
a, b – model of a hollow shaft after rolling

According to the results of numerical modeling we conducted physical modeling of the rolling process for a hollow shaft using the TRV-320 screw-cutting lathe on the scale of 1:2. Wood's alloy was selected as a modeling material. The results of physical modeling are shown in Fig. 8.

Conclusion

The analysis of the findings obtained through physical and numerical modeling confirmed the possibility of using chromium steel alloy grade 11H11N2V2MF-Sh for manufacturing a hollow shaft with a tapered cylinder. It was established that the most difficult problem to be solved in the design process is to avoid deformation at the junction between the flat and the conical parts of the shaft. As shown in the article, this problem can be solved by increasing the thickness of the initial workpiece; it has a positive effect on the distribution of internal stress, and increases the compressive stress, by either local thickening of the workpiece at the junction between the flat and conical parts, or local cooling to increase metal flow stress in that location. In addition, for the manufacture of a shaft with a small cone angle it is necessary to use a pre-deformed workpiece, which is similar in shape to the manufactured shaft.

Thus, increasing the thickness of the initial workpiece has a positive effect on the distribution of internal stress, however, it results in significant loads on the deforming roller and other equipment components. Using the pre-deformed workpiece can significantly increase the productivity of the process. The use of multiple rolling in several passes will provide significant reduction in the energy-power parameters of the equipment.

Acknowledgment

The work was supported by the Russian Ministry of Education, in the framework of the Federal Target Program "Research and development on priority directions of scientific-technological complex of Russia for 2014-2020" (Agreement # 14.604.21.0091 of July 8, 2014, a unique project identifier RFMEFI60414X0091).

References

1. Utyashev, F. Z., et al. (2013). Scientific fundamentals of high-efficiency roll forming technology for axially symmetrical parts of a gas-turbine engine rotor of high-temperature alloy. *Journal of Machinery Manufacture and Reliability*, 42 (5), 419-426. (Rus)

2. Wong, C. C., Dean, T. A., & Lin, J. (2003). A review of spinning, shear forming and flow forming processes. *International Journal of Machine Tools and Manufacture*. 43 (14), 1419-1435.

3. Muhtarov Sh.H., et.al. (2013). Razrabotka processa rotacionnoj vytjazhki konicheskih detalej iz listovogo materiala [Development of rotary drawing of conical parts from sheet material]. Perspektivnye materialy [Advanced Materials]. Spec. vyp. (15), 92-96. (Rus)

4. Xia, Q., et al. (2005). A study of the one-path deep drawing spinning of cups. *Journal of Materials Processing Technology*. 159 (3), 397-400.

5. Hua, F. A., et al. (2005). Three-dimensional finite element analysis of tube spinning. *Journal of Materials Processing Technology*. 168 (1), 68-74.

6. Mohebbi, M. S., & Akbarzadeh, A. (2010). Experimental study and FEM analysis of redundant strains in flow forming of tubes. *Journal of Materials Processing Technology*. 210 (2), 389-395.

7. Zhan, M., et al. (2007). 3D FEM analysis of influence of roller feed rate on forming force and quality of cone spinning.*Journal of Materials Processing Technology*. (187), 486-491.

8. Suhorukov, R.Ju., et al. (2015). Opredelenie silovyh parametrov processa izotermicheskoj raskatki otvetstvennyh detalej gazoturbinnyh dvigatelej [Determination of force parameters of isothermal rolling of gas turbine engines critical parts]. Problemy mashinostroenija i avtomatizacii [Problems of mechanical engineering and automation]. 1, 116-122.

9. Aljushin, Ju. A. (1997). Mehanika processov deformacii v prostranstve peremennyh Lagranzha [The mechanics of deformation processes in the space of Lagrange variables]. – M.: Mashinostroenie. (Rus)

10.Davey, K. & Ward, M. J. (2003). An ALE approach for finite element ring-rolling simulation of profiled rings. *Journal of Materials Processing Technology*. 139 (1), 559-566.

11.Cockcroft, M. G. & Latham, D. J. (1968). Ductility and the workability of metals. *J Inst Metals*. 96 (1), 33-39.

12.Umbrello, D. (2008). Finite element simulation of conventional and high speed machining of Ti6Al4V alloy. *Journal of materials processing technology*. 196 (1), 79-87.

13.Ko, D.C., Kim, B.M. & Choi, J.C. (1996). Prediction of surface-fracture initiation in the axisymmetric extrusion and simple upsetting of an aluminum alloy. *Journal of materials processing technology*. 62 (1), 166-174.

14.Landre, J. et al. (2003). On the utilisation of ductile fracture criteria in cold forging. *Finite elements in analysis and design*. 39 (3), 175-186.